

Electron attachment to perfluorocarbon compounds. I. *c*-C₄F₆, 2-C₄F₆, 1,3-C₄F₆, *c*-C₄F₈ and 2-C₄F₈^{a)}

A. A. Christodoulides,^{b)} L. G. Christophorou,^{c)} R. Y. Pai, and C. M. Tung^{d)}

Atomic, Molecular and High Voltage Physics Group, Health and Safety Research Division, Oak Ridge National Laboratory, Oak Ridge, Tennessee 37830

(Received 23 August 1978)

Electron attachment rates αw , as a function of the pressure-reduced electric field E/P_{298} and mean electron energy $\langle \epsilon \rangle$ have been measured for trace amounts ($<10^{-3}$ Torr) each of *c*-C₄F₆ (perfluorocyclobutene), 2-C₄F₆ (perfluoro-2-butyne), 1,3-C₄F₆ (perfluoro-1,3-butadiene), *c*-C₄F₈ (perfluorocyclobutane), and 2-C₄F₈ (perfluoro-2-butene) in mixtures with N₂ (pressures 500–2000 Torr) and Ar (pressures 500–1500 Torr) at $T = 298^\circ\text{K}$. The thermal attachment rates for these molecules were found to be 4.89×10^9 , 1.77×10^9 , 4.26×10^9 , 4.05×10^8 , and $1.56 \times 10^9 \text{ sec}^{-1} \text{ Torr}^{-1}$, respectively. From the $\alpha w(\langle \epsilon \rangle)$ data, the attachment cross sections $\sigma_a(\epsilon)$ as a function of electron energy ϵ have been determined using the swarm-unfolding technique and are reported. For all five perfluorocarbon molecules, $\sigma_a(\epsilon)$ are very large. They exhibit three distinct negative ion resonances with maxima at: ~ 0.0 , 0.19, and 0.80 eV for 2-C₄F₆; ~ 0.0 , 0.17, and 1.04 eV for 1,3-C₄F₆; ~ 0.0 , 0.22, and 0.48 eV for *c*-C₄F₈; and ~ 0.0 , 0.18, and 0.59 eV for 2-C₄F₈. For *c*-C₄F₆, only a shoulder with a possible maximum at ~ 0.14 eV was observed, in addition to the maxima at ~ 0.0 and 0.71 eV. Although the positions of the maxima in $\sigma_a(\epsilon)$ vary only slightly among these compounds, the magnitude of $\sigma_a(\epsilon)$ depends strongly on structure.

I. INTRODUCTION

Electron attachment studies are of fundamental importance in the development of a basic understanding of molecules and their interactions with slow electrons. They are also of a considerable practical interest. For example, perfluorinated hydrocarbons have a potential use as high voltage gaseous insulators (see, for example, Refs. 1 to 4 for recent work). The high breakdown strength of these gases is principally ascribed to their high electron attachment cross sections at low energies, as is discussed in this and the following paper (Part II). However, there is little quantitative information in the literature concerning their electron attachment properties in the energy range from thermal to ~ 3 eV.

In this paper (Part I), we report on and discuss the capture of slow ($\lesssim 3$ eV) electrons by the perfluorocarbons *c*-C₄F₆, 2-C₄F₆, 1,3-C₄F₆, *c*-C₄F₈, and 2-C₄F₈. The determination of the magnitude of the thermal electron attachment rate, the magnitude and energy dependence of the electron attachment rate and cross section, the position of the negative ion resonance states below ~ 1.4 eV, the possible reaction mechanisms for formation and dissociation of the parent negative ions, and the effect of molecular structure on the electron capture processes at low energies are the principal concerns of this work.

II. EXPERIMENTAL SECTION

The electron-swarm method employed in the present study has been described in detail earlier.^{5–7} All mea-

surements were performed at room temperature ($T = 298^\circ\text{K}$). The carrier gases N₂ and Ar were used at pressures ranging from 500 to 2000 torr and from 500 to 1500 torr, respectively, and were of the highest purity available. The pressure ranges of the perfluorocarbons (C₄F_x or PFC) investigated are given in Table I. All compounds were provided by Columbia Organic Chemicals Company with a guaranteed purity of $>97\%$. The PFC molecules attach electrons very strongly (see Sec. IV) and for this reason minute amounts of these compounds had to be used in the experiments. In order to increase the accuracy of the pressure measurements, an expansion procedure was employed whereby the attaching gas was introduced into a small volume at higher pressure and then expanded into the experimental chamber. The ratio of the volume of the experimental (main) chamber to the auxiliary chamber was 520:1. Bake-out facilities were provided to remove possible adsorbed gases on the walls of the chamber and the gas manifold. A vacuum of $\sim 3 \times 10^{-8}$ torr was usually reached in the experimental chamber prior to the introduction of the PFC gases.

The possible errors in our measurements are both systematic and random.

Systematic errors. There are three sources of systematic errors: the electrode separation distance (electron drift distance), the voltage applied to the electrodes, and the presence of impurities. The electrode separation can be measured to better than $\pm 0.5\%$. The applied voltage is measured by a calibrated digital voltmeter to $\pm 0.01\%$. Impurities due to outgassing are negligible, since we routinely pumped the vacuum system to 10^{-8} torr before introduction of the gas in the experimental chamber.

The major source of systematic uncertainty is due to any impurities in the sample, as supplied by the manufacturer. All compounds were better than 97% pure. The error introduced by impurities is usually large when the studied compound attaches electrons

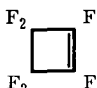
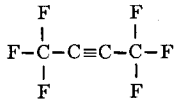
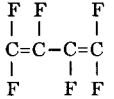
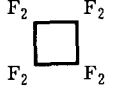
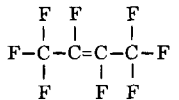
^{a)} Research sponsored by the Division of Electric Energy Systems of the U. S. Department of Energy under contract (W-7405-eng-26) with Union Carbide Corporation.

^{b)} Visiting Scientist; Permanent address, Department of Physics, University of Ioannina, Ioannina, Greece.

^{c)} Also Department of Physics, University of Tennessee, Knoxville, TE 37916.

^{d)} Postdoctoral Fellow.

TABLE I. Nomenclature, structural formulas, pressure ranges used, and boiling and freezing points for $c\text{-C}_4\text{F}_6$, $2\text{-C}_4\text{F}_6$, $1, 3\text{-C}_4\text{F}_6$, $c\text{-C}_4\text{F}_8$, and $2\text{-C}_4\text{F}_8$.

Perfluorocarbon	Molecular formula	Structural formula	$P_{\text{C}_x\text{F}_y}$ in N_2^a (10^{-5} torr)	$P_{\text{C}_x\text{F}_y}$ in Ar^b (10^{-5} torr)	Boiling point ($^{\circ}\text{C}$)	Freezing point ($^{\circ}\text{C}$)
Perfluorocyclobutene	$c\text{-C}_4\text{F}_6$		(15) ^c 4.3–88.4	(9) 42.7–146.1	0 ^d 1.13 ^f 3 ^e	–60 ^e –60.4 ^f –61 ^d
Perfluoro-2-butyne	$2\text{-C}_4\text{F}_6$		(11) 6.0–12.0	(4) 7.6–9.5	–24 to –23 ^g –24.6 ^e –25 ^h	–117.4 ^e
Perfluoro-1,3-butadiene	$1, 3\text{-C}_4\text{F}_6$		(8) 6.7–9.6	(5) 9.2–14.0	6.0 ^d 6.0 ^e 6.6 ^f	–132 ^d –132.4 ^e
Perfluorocyclobutane	$c\text{-C}_4\text{F}_8$		(8) 8.0–16.0	(4) 8.0–14.0	–4 ^e –5 ^f –6 ⁱ	–38.7 ^e –40 ^f –41.0 ⁱ
Perfluoro-2-butene	$2\text{-C}_4\text{F}_8$		(11) 8.0–12.0	(8) 8.0–14.0	0.4 to 3.0 ^f	–129 to –139 ^f

^aThe pressures of N_2 employed are 500, 1000, 1500, and 2000 torr.^bThe pressures of Ar employed are 500, 1000, and 1500 torr.^cThe numbers in parentheses give the number of independent runs made in N_2 or Ar .^dJ. H. Simons and T. J. Brice, *Fluorine Chemistry*, edited by J. H. Simons (Academic, New York, 1954), Vol. II, Chap. 6, p. 405.^eHandbook of Chemistry and Physics (Chemical Rubber, Cleveland, 1974–1975), 55th Edition, p. C-75.^fW. H. Pearlson, *Fluorine Chemistry*, edited by J. H. Simons (Academic, New York, 1950), Vol. I, Chap. 14, p. 500.^gT. J. Brice, *Fluorine Chemistry*, edited by J. H. Simons (Academic, New York, 1950), Vol. I, Chap. 13, p. 452.^hE. R. Larsen, *Fluorine Chem. Rev.* 3, 1 (1969).ⁱH. G. Bryce, *Fluorine Chemistry*, edited by J. H. Simons (Academic, New York, 1964), Vol. V, Chap. 4, p. 347.

weakly and the impurities strongly. The perfluorocarbons investigated in this work, however, have very large electron attachment rates, over a wide electron energy range. Thus, it is anticipated that any error due to impurities is $\leq 3\%$.

Random errors. Errors in measurements of the total and especially partial pressures, uncertainties in extrapolation of the peak pulse height at zero time⁷ (initial time of introduction of attaching gas in the experimental chamber) for all E/P values used, and recording the peak of the pulse height distribution are sources of random error which are reflected in the variation of the measured attachment rates from run to run.

The attachment rates that we measure fall within an envelope of 10% of the average values given in Tables II and III (see Sec. IV. B). This spread is primarily due to uncertainties in the pressure measurement of PFC. It is emphasized that the random contribution of error does not affect the relative attachment cross sections that we unfold (see Sec. III. B). Unfolding the $\alpha w(\langle\epsilon\rangle)$ functions from a single run gives the same relative cross section as the unfolding of an average set of αw values obtained from many runs.

III. BASIS OF MEASUREMENTS AND CALCULATIONS

A. The electron energy distribution function $f(\epsilon, E/P)$

In the electron swarm method, the electron attachment rate αw (α is the electron attachment coefficient in $\text{cm}^{-1}\text{torr}^{-1}$ and w is the electron drift velocity in cm sec^{-1}) for a gas is measured as a function of the pressure-reduced electric field E/P (in units of $\text{V cm}^{-1}\text{torr}^{-1}$) at constant temperature T . For every value of E/P , the distribution of electron energies $f(\epsilon, E/P)$ in the electron swarm depends strongly on the gas under study. The $f(\epsilon, E/P)$ are unknown for the PFC's investigated. To overcome this difficulty, our experiments were performed on binary gas mixtures, where the perfluorocarbon under study was mixed with the nonelectron attaching gas N_2 or Ar for which $f(\epsilon, E/P)$ are known^{5,7,8} over a suitable range of E/P values. Knowledge of $f(\epsilon, E/P)$ or $f(\epsilon, \langle\epsilon\rangle)$, where $\langle\epsilon\rangle$ is the mean electron energy, is necessary for a meaningful physical analysis of the raw experimental electron attachment data (see Sec. IV. C).

The compounds under investigation were mixed in very small proportions with the carrier gases (see Table I). This ensured that $f(\epsilon, E/P)$ in the mixture

TABLE II. Electron attachment rates for $c\text{-C}_4\text{F}_6$, $2\text{-C}_4\text{F}_6$, $1,3\text{-C}_4\text{F}_6$, $c\text{-C}_4\text{F}_8$, and $2\text{-C}_4\text{F}_8$ in N_2 .

E/P_{298} (V cm ⁻¹ torr ⁻¹)	$\langle\epsilon\rangle$ (eV)	αw in N_2 (10 ⁹ sec ⁻¹ torr ⁻¹)					$(\alpha w)_{\text{max}}^a$ (10 ⁹ sec ⁻¹ torr ⁻¹)
		$c\text{-C}_4\text{F}_6$	$2\text{-C}_4\text{F}_6$	$1,3\text{-C}_4\text{F}_6$	$c\text{-C}_4\text{F}_8$	$2\text{-C}_4\text{F}_8$	
0.02	0.046	4.20	1.69	3.85	0.45	1.48	13.25
0.03	0.054	3.73	1.60	3.55	0.48	1.40	12.55
0.04	0.064	3.30	1.53	3.28	0.54	1.34	11.44
0.05	0.075	2.98	1.49	3.10	0.61	1.30	10.60
0.06	0.087	2.68	1.43	2.93	0.67	1.25	9.70
0.07	0.099	2.45	1.40	2.79	0.76	1.21	9.05
0.10	0.131	1.97	1.34	2.53	0.93	1.17	7.85
0.15	0.181	1.47	1.29	2.20	1.14	1.10	6.60
0.20	0.230	1.14	1.27	1.92	1.25	1.03	5.85
0.25	0.285	0.94	1.28	1.70	1.31	0.98	5.30
0.35	0.376	0.67	1.33	1.35	1.31	0.89	4.60
0.50	0.490	0.46	1.36	1.03	1.20	0.77	3.97
0.60	0.550	0.40	1.38	0.91	1.13	0.73	3.72
0.80	0.646	0.30	1.38	0.75	1.01	0.64	3.40
1.00	0.715	0.26	1.33	0.68	0.91	0.59	3.20
1.20	0.764	0.23	1.27	0.62	0.84	0.54	3.08
1.40	0.803	0.20	1.22	0.57	0.77	0.50	3.00
1.70	0.846	0.17	1.15	0.52	0.71	0.46	2.93

^aThe values of $(\alpha w)_{\text{max}}$ were obtained using Eq. (9) and the $f_{\text{N}_2}(\epsilon, \langle\epsilon\rangle)$ functions for N_2 (see Sec. III. D).

remained basically unchanged, characteristic of the carrier gas alone.

B. The electron attachment cross section $\sigma_a(\epsilon)$

The rate $\alpha w(E/P)$ of electron attachment to a molecule is related to the electron attachment cross section $\sigma_a(\epsilon)$ (in units of cm²) and $f(\epsilon, E/P)$ by

$$\alpha w(E/P) = N_0 \left(\frac{2}{m} \right)^{1/2} \int_0^\infty \epsilon^{1/2} \sigma_a(\epsilon) f(\epsilon, E/P) d\epsilon. \quad (1)$$

In Eq. (1), $N_0 (= 3.241 \times 10^{16})$ is the number of electron attaching molecules per cm³ per torr at 298°K, and m is the electron mass.

Two techniques have been developed for the determination of $\sigma_a(\epsilon)$ from electron-swarm experiments via Eq. (1): the swarm-beam⁹ and the swarm unfolding¹⁰

techniques. In the former, $\sigma_a(\epsilon)$ is obtained through a combination of the measured $\alpha w(\langle\epsilon\rangle)$ data from electron-swarm experiments with the measured negative ion yield $I(\epsilon)$ data from electron-beam experiments. In the latter, which is the one employed in the present study, $\sigma_a(\epsilon)$ is determined from the $\alpha w(\langle\epsilon\rangle)$ data alone and this can be done virtually at any gas density for which $f(\epsilon, E/P)$ is known and $\alpha w(\langle\epsilon\rangle)$ has been measured over a wide and convenient range of E/P . The rate αw is a quantity which is averaged over $f(\epsilon, E/P)$. Hence, we may write

$$\alpha w(\langle\epsilon\rangle_j) = \int_0^\infty \alpha w(\epsilon) f(\epsilon, \langle\epsilon\rangle_j) d\epsilon, \quad (2)$$

where $\alpha w(\langle\epsilon\rangle_j)$ is the experimentally measured value of αw at the mean electron energy $\langle\epsilon\rangle_j$ (i. e., at the j th value of E/P), $f(\epsilon, \langle\epsilon\rangle_j)$ is the electron energy distribu-

TABLE III. Electron attachment rates for $c\text{-C}_4\text{F}_6$, $2\text{-C}_4\text{F}_6$, $1,3\text{-C}_4\text{F}_6$, $c\text{-C}_4\text{F}_8$, and $2\text{-C}_4\text{F}_8$ in Ar.

E/P_{298} (V cm ⁻¹ torr ⁻¹)	$\langle\epsilon\rangle$ (eV)	αw in Ar (10 ⁸ sec ⁻¹ torr ⁻¹)					$(\alpha w)_{\text{max}}^a$ (10 ⁸ sec ⁻¹ torr ⁻¹)
		$c\text{-C}_4\text{F}_6$	$2\text{-C}_4\text{F}_6$	$1,3\text{-C}_4\text{F}_6$	$c\text{-C}_4\text{F}_8$	$2\text{-C}_4\text{F}_8$	
0.010	0.498		12.39	9.57	11.32	7.67	38.90
0.015	0.570		13.39	8.33	10.47	7.27	36.33
0.02	0.641	2.68	13.61	7.50	9.63	6.86	33.92
0.03	0.752	2.22	13.29	6.67	8.20	5.97	31.32
0.04	0.848	1.88	12.22	5.78	7.03	5.16	29.00
0.05	0.935	1.62	11.08	5.23	6.08	4.52	28.14
0.06	1.012	1.41	9.99	4.70	5.30	4.04	27.04
0.10	1.285	0.97	7.26	3.47	3.77	2.80	23.76
0.15	1.559	0.71	5.44	2.63	2.67	2.08	21.12
0.20	1.797	0.58	4.40	2.20	2.08	1.66	18.70
0.25	2.008	0.48	3.77	1.90	1.76	1.38	16.65
0.30	2.197	0.44	3.32	1.70	1.53	1.22	14.98
0.40	2.526	0.36	2.75	1.40	1.24	0.98	12.51
0.50	2.808	0.30	2.26	1.20	1.04	0.82	10.81

^aThe values of $(\alpha w)_{\text{max}}$ were obtained using Eq. (9) and the $f_{\text{Ar}}(\epsilon, \langle\epsilon\rangle)$ functions for Ar (see Sec. III. D).

tion function that corresponds to $\langle\epsilon\rangle_j$, and $\alpha w(\epsilon)$ is the value of the monoenergetic attachment rate at the electron energy ϵ (i. e., the value of the attachment rate that would be measured, if all the electrons in the swarm had the same energy ϵ). Equation (2) forms the basis of the swarm unfolding technique. Christophorou *et al.*¹⁰ have described an iterative procedure which allows $\alpha w(\epsilon)$ to be unfolded from the measured $\alpha w(\langle\epsilon\rangle_j)$ using the corresponding known $f(\epsilon, \langle\epsilon\rangle_j)$ functions. Once $\alpha w(\epsilon)$ is determined, $\sigma_a(\epsilon)$ is obtained from

$$\sigma_a(\epsilon) = \frac{\alpha w(\epsilon)}{N_0(2/m)^{1/2}\epsilon^{1/2}} = 5.225 \times 10^{-25} \frac{\alpha w(\epsilon)}{\epsilon^{1/2}}, \quad T = 298^\circ\text{K}. \quad (3)$$

In Eq. (3), the units of $\sigma_a(\epsilon)$ are in cm^2 and the units of ϵ in eV.

The number of iterations required for convergence of the $\alpha w(\epsilon)$ functions is usually ~ 1000 , although in the present study we have always performed ~ 3000 iterations. The extent to which the experimental $[\alpha w(\langle\epsilon\rangle_j)]_{\text{exptl.}}$ and the calculated $[\alpha w(\langle\epsilon\rangle_j)]_{\text{calc.}}$ values agree can be assessed from the value of the ratio R , defined as

$$R = \frac{\sum_j \{[\alpha w(\langle\epsilon\rangle_j)]_{\text{exptl.}} - [\alpha w(\langle\epsilon\rangle_j)]_{\text{calc.}}\}^2}{\sum_j [\alpha w(\langle\epsilon\rangle_j)]_{\text{exptl.}}^2}. \quad (4)$$

The lower the value of R , the better the overall agreement between the experimental and the calculated $\alpha w(\langle\epsilon\rangle_j)$ values, and hence the closer is the final function $\alpha w(\epsilon)$ to the true monoenergetic attachment rate. In all cases considered in this paper, R was $\sim 10^{-5}$.

C. The maximum electron attachment cross section

$$\sigma_{a, \text{max}} (= \pi \lambda^2)$$

The integral electron scattering or reaction cross section σ_{ba} for a spherically symmetric potential field is¹¹

$$\sigma_{ba} = \frac{\pi}{k^2} \sum_l (2l+1) |S_{ba} - \delta_{ba}|^2, \quad (5)$$

where $k = 2\pi/\lambda = 1/\lambda$ is the wave number for the incoming wave (λ is the de Broglie wavelength of the electron), $l(=0, 1, 2, 3, \dots)$ is the angular momentum quantum number, S_{ba} is the scattering matrix for the initial state a and the final state(s) b , δ_{ba} is a delta function of the energy of these states, and the reduced mass of the system was taken equal to the electron mass.

The sum of all reaction cross sections over all possible final channels $b(\neq a)$ (i. e., the total reaction cross section σ_r) is¹¹

$$\sigma_r = \frac{\pi}{k^2} \sum_{b \neq a} \sum_{l=0}^{\infty} (2l+1) |S_{ba}|^2 = \frac{\pi}{k^2} \sum_{l=0}^{\infty} (2l+1) (1 - |S_{aa}|)^2. \quad (6)$$

S_{aa} expresses the matrix elements when only elastic scattering takes place.

The maximum value $(\sigma_r)_{\text{max}, l}$ of the partial reaction cross section for given l is obtained from Eq. (6):

$$(\sigma_r)_{\text{max}, l} = \frac{\pi}{k^2} (2l+1). \quad (7)$$

For a slow electron, the effective range of electron-molecule interaction is small compared with the electron de Broglie wavelength, and it can be assumed that only s waves ($l=0$) participate in the scattering. Thus, from Eq. (7), we have

$$\sigma_{a, \text{max}} (= (\sigma_r)_{\text{max}, l=0}) = \frac{\pi}{k^2} = \pi \lambda^2 = \frac{1.197 \times 10^{-15}}{\epsilon(\text{in eV})} \text{cm}^2. \quad (8)$$

In low-energy electron-swarm experiments, this can be considered to be the maximum (s -wave) electron capture cross section. Experimental $\sigma_a(\epsilon)$ are compared in Sec. IV.D with $\sigma_{a, \text{max}}$ at various values of the incident electron energy ϵ . It is apparent from these results that the measured $\sigma_a(\epsilon)$ are large, often $\gtrsim 50\%$ of $\pi \lambda^2$ (see Figs. 8 and 9).

D. The maximum electron attachment rate $[\alpha w(\langle\epsilon\rangle)]_{\text{max}}$

To make a more direct comparison of the theoretical maximum (s -wave) electron capture rate with the experimental results, we determined through Eqs. (1) and (8) the maximum electron attachment rate as a function of $\langle\epsilon\rangle$, viz.,

$$\begin{aligned} [\alpha w(\langle\epsilon\rangle)]_{\text{max}} &= N_0 \left(\frac{2}{m}\right)^{1/2} \left(\frac{\pi \hbar^2}{2m}\right) \int_0^\infty \epsilon^{-1/2} f(\epsilon, \langle\epsilon\rangle) d\epsilon \\ &= 2.301 \times 10^9 \int_0^\infty \epsilon^{-1/2} f(\epsilon, \langle\epsilon\rangle) d\epsilon \quad (\text{sec}^{-1} \text{torr}^{-1}), \end{aligned} \quad (9)$$

where N_0 is the gas number density at $T = 298^\circ\text{K}$.

In the present work, the known^{5,7,8} $f(\epsilon, \langle\epsilon\rangle)$ functions for N_2 and Ar were used in the energy range of interest. A plot of $[\alpha w(\langle\epsilon\rangle)]_{\text{max}}$ as a function of $\langle\epsilon\rangle$ would lie above the experimentally measured $\alpha w(\langle\epsilon\rangle)$ values. The values for $[\alpha w(\langle\epsilon\rangle)]_{\text{max}}$ for N_2 and Ar are listed in Tables II and III, respectively (see Sec. IV. C).

E. The thermal electron attachment rate $(\alpha w)_{\text{ther}}$

The thermal value of the electron attachment rate for a molecule is an important parameter that many workers tried to obtain using a variety of experimental techniques (see Sec. V. D). For example, it is this parameter which is often used^{12,13} in comparisons of gaseous- and liquid-phase data on electron attachment. For many molecules, however, this quantity is uncertain due mainly to impurities, pressure dependencies, and nonthermal conditions for the electrons. As a rule,^{12,14} two or more electron attachment resonances exist below ~ 1 eV, often within a few tenths of 1 eV of thermal energy, which further complicates such determinations.

The thermal electron attachment rate can be determined in electron-swarm studies by (i) direct measurement at $E/P = 0$, which is practically not possible, and (ii) indirectly from αw vs E/P plots by extrapolation of the lower E/P attachment rate data to $E/P = 0$.

A third method for determining $(\alpha w)_{\text{ther}}$ has been suggested.¹² The monoenergetic attachment rate $\alpha w(\epsilon)$, as determined from the experimental $\alpha w(\langle\epsilon\rangle)$ data (see Sec. III. B) was used to obtain $(\alpha w)_{\text{ther}}$, viz.,

$$(\alpha w)_{\text{ther}} = \int_0^\infty \alpha w(\epsilon) f_M(\epsilon) d\epsilon, \quad (10)$$

where $f_M(\epsilon) = N_0 [2/\pi^{1/2} (kT)^{3/2}] \epsilon^{1/2} e^{-(\epsilon/kT)}$ is the Maxwellian electron energy distribution function at $T = 298^\circ\text{K}$. The determination of $(\alpha w)_{\text{ther}}$ in this way constitutes an accurate and convenient method, since measurement of αw for truly thermal electrons is rather difficult to make directly and accurately.

F. The energy integrated electron attachment cross section $\int_{\epsilon_1}^{\epsilon_2} \sigma_a(\epsilon) d\epsilon$

There are certain basic and applied areas, such as the field of gaseous dielectrics, where electron capture processes are of great importance (see Part II). In these cases, a comparison of the electron attaching efficiencies of molecules in a particular energy range in relation to each other and to $\sigma_{a,\text{max}}$ are most useful quantities. We thus introduce the ratio

$$RI_{\epsilon_1}^{\epsilon_2} \equiv \left[\frac{\int_{\epsilon_1}^{\epsilon_2} \sigma_a(\epsilon) d\epsilon}{\int_{\epsilon_1}^{\epsilon_2} \pi \chi^2 d\epsilon} \right] \quad (11)$$

of the integrated cross sections for capture of electrons with energies between ϵ_1 and ϵ_2 . [Such ratios can be obtained from plots of $\sigma_a(\epsilon)$ vs ϵ (see Table V)], and the ratio of the integrated electron attachment rates

$$RI_{\epsilon_1}^{\epsilon_2} \equiv \left\{ \frac{\int_{\epsilon_1}^{\epsilon_2} \alpha w(\langle \epsilon \rangle) d\langle \epsilon \rangle}{\int_{\epsilon_1}^{\epsilon_2} [\alpha w(\langle \epsilon \rangle)]_{\text{max}} d\langle \epsilon \rangle} \right\}. \quad (12)$$

In practical applications (see Part II), where the removal of electrons via attachment is desirable, Eqs. (11) and (12) can provide useful information although it should be kept in mind that it is the overlap of $\sigma_a(\epsilon)$ and

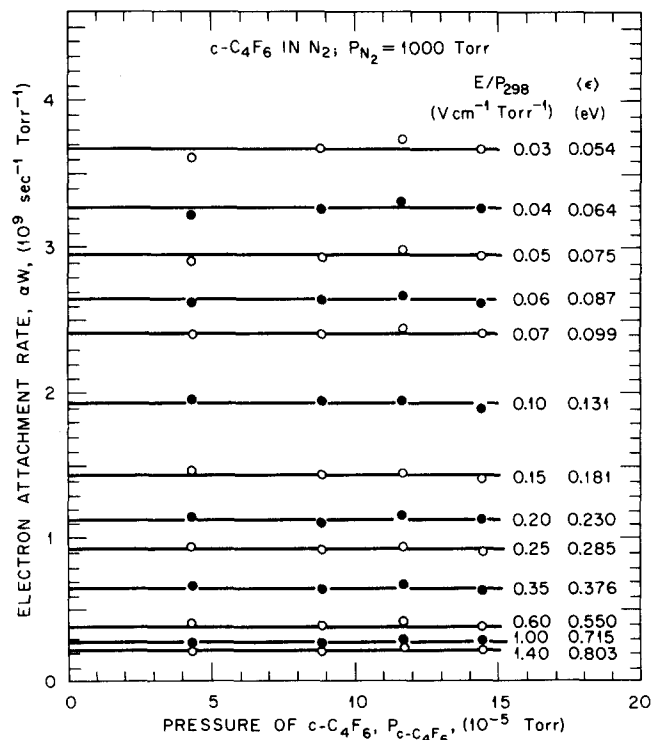


FIG. 1. Electron attachment rate αw vs attaching gas pressure $P_{c-C_4F_6}$, for $c-C_4F_6$ in N_2 ($P_{N_2} = 1000$ torr) for a number of E/P_{298} values (or $\langle \epsilon \rangle$ values).

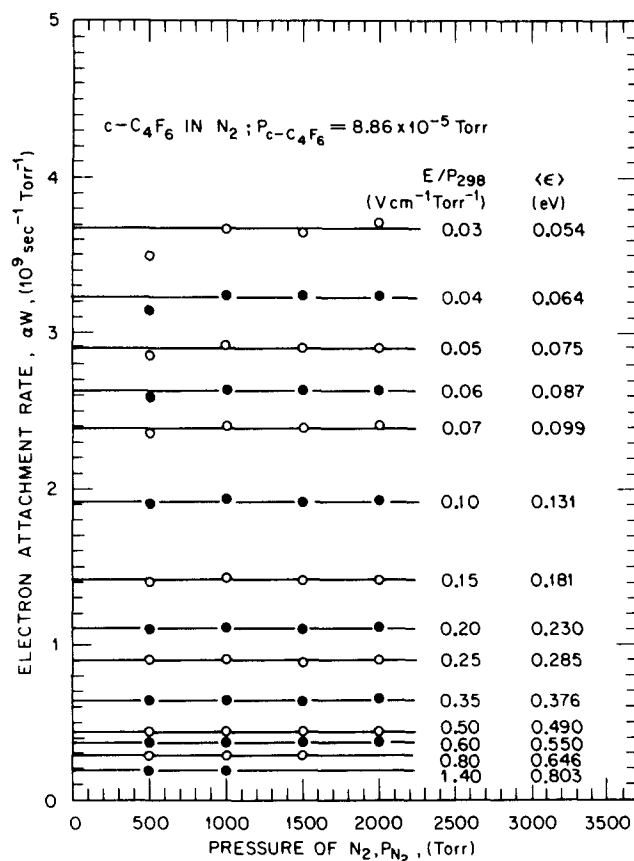


FIG. 2. Electron attachment rate αw vs pressure P_{N_2} , of N_2 for $c-C_4F_6$ ($P_{c-C_4F_6} = 8.86 \times 10^{-5}$ torr) for a number of E/P_{298} values (or $\langle \epsilon \rangle$ values).

$f(\epsilon, E/P)$ which is the most important quantity, i. e., $\int_0^\infty \sigma_a(\epsilon) f(\epsilon, E/P) d\epsilon$.

IV. EXPERIMENTAL RESULTS

A. Electron attachment rates as a function of partial and total pressure

The electron attachment rates for the five perfluorocarbons $c-C_4F_6$, $2-C_4F_6$, $1,3-C_4F_6$, $c-C_4F_8$, and $2-C_4F_8$ investigated were found to be independent of the attaching gas pressure $P_{C_xF_y}$ at constant carrier gas pressure and E/P . The $P_{C_xF_y}$ ranged from 4.3×10^{-5} to 1.46×10^{-3} torr (see Table I). As an example, the αw data for $c-C_4F_6$ are plotted in Fig. 1 as a function of $P_{c-C_4F_6}$ at $P_{N_2} = 1000$ torr. No partial pressure dependence at any E/P value is seen.

The $\alpha w(E/P)$ functions were found also to be independent of the carrier gas pressure P_{N_2} or P_{Ar} in the range of 500 to 2000 torr at constant $P_{C_xF_y}$ and E/P . An example of $\alpha w(E/P)$ vs P_{N_2} is given in Fig. 2 for $P_{c-C_4F_6} = 8.86 \times 10^{-5}$ torr and for various values of E/P .

The attachment rates reported in this paper are those averaged over a number of experimental runs at various attaching and carrier gas pressures as listed in Table I.

B. Electron attachment rates as a function of E/P

In Fig. 3 is shown the dependence of αw on E/P for $c-C_4F_6$ (○), $2-C_4F_6$ (●), and $1,3-C_4F_6$ (▲) in mixtures

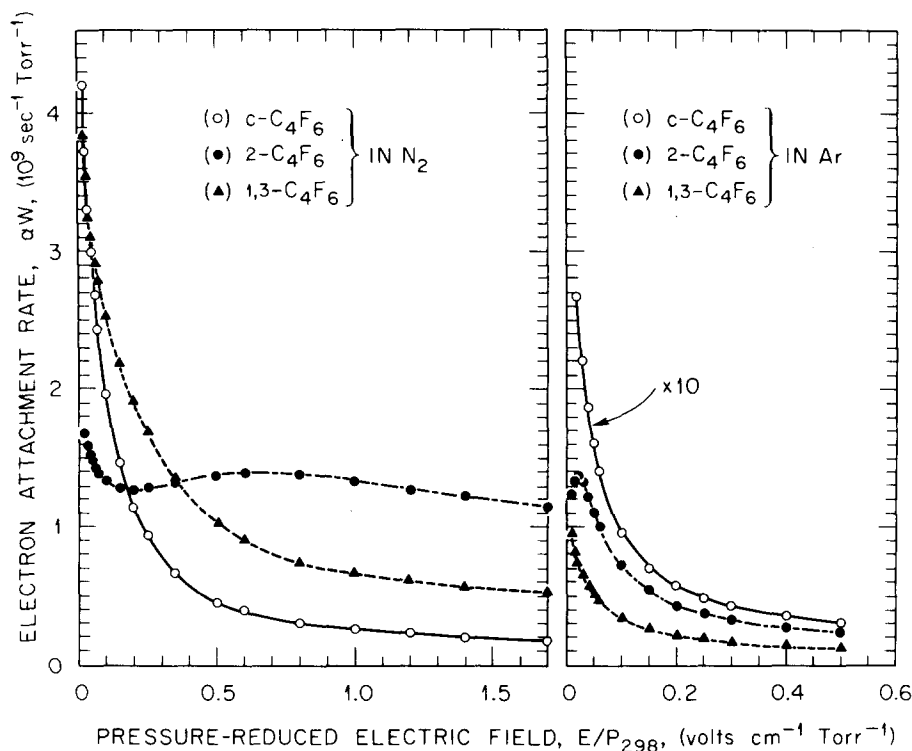


FIG. 3. Electron attachment rate αw vs E/P_{298} for $c\text{-C}_4\text{F}_6$ (○), $2\text{-C}_4\text{F}_6$ (●), and $1,3\text{-C}_4\text{F}_6$ (▲) in N_2 and Ar. Note that the data for $c\text{-C}_4\text{F}_6$ in Ar were multiplied by a factor of 10 for convenience of display.

with N_2 and Ar. Similar results for $c\text{-C}_4\text{F}_8$ (Δ) and $2\text{-C}_4\text{F}_8$ (■) in N_2 and Ar are shown in Fig. 4.

The main features of the $\alpha w(E/P)$ functions in Figs. 3 and 4 are the maxima at $E/P \approx 0.3 \text{ V cm}^{-1} \text{ torr}^{-1}$ for $c\text{-C}_4\text{F}_8$ and at $E/P \approx 0.7 \text{ V cm}^{-1} \text{ torr}^{-1}$ for $2\text{-C}_4\text{F}_8$ in N_2 . The αw values for $c\text{-C}_4\text{F}_8$, $1,3\text{-C}_4\text{F}_8$, and $2\text{-C}_4\text{F}_8$ are increasing as E/P decreases, and remain high ($\geq 1 \times 10^8 \text{ sec}^{-1} \text{ torr}^{-1}$) for all five perfluorocarbons, even at the highest E/P values used. The measured values of αw for $c\text{-C}_4\text{F}_8$, $2\text{-C}_4\text{F}_8$, $1,3\text{-C}_4\text{F}_8$, $c\text{-C}_4\text{F}_6$, and $2\text{-C}_4\text{F}_6$ in N_2 and Ar are listed, respectively, in Tables II and III as functions of both E/P and $\langle \epsilon \rangle$.

C. Electron attachment rates as a function of $\langle \epsilon \rangle$

Although it is customary to plot the experimental data on αw as a function of E/P for each carrier gas used,

a plot of αw vs $\langle \epsilon \rangle$ is more meaningful, since the latter should be independent of the carrier gas. Tabulated $\langle \epsilon \rangle$ values as a function of E/P for the carrier gases C_2H_4 , N_2 (Ref. 15), and Ar were reported^{5,7,8} earlier.

In Fig. 5, αw vs $\langle \epsilon \rangle$ plots are presented for $c\text{-C}_4\text{F}_8$, $2\text{-C}_4\text{F}_8$, and $1,3\text{-C}_4\text{F}_8$. The "open" points are data taken with N_2 as the carrier gas at 500, 1000, 1500, and 2000 torr, and the "solid" points are data taken with Ar as the carrier gas at 500, 1000, and 1500 torr. They are averages of 15, 11, and 8 runs in N_2 and 9, 4, and 5 runs in Ar, respectively, for $c\text{-C}_4\text{F}_8$ (□, ■), $2\text{-C}_4\text{F}_8$ (○, ●), and $1,3\text{-C}_4\text{F}_8$ (Δ, ▲). The theoretical maximum electron attachment rate (Sec. III. D) is also shown in Fig. 5 as a function of $\langle \epsilon \rangle$ using $f(\epsilon, E/P)$ for N_2 (◇) and Ar (◆). In the same figure, the calculated thermal electron attachment rate at $\langle \epsilon \rangle = \frac{3}{2} kT_{298} \approx 0.038$

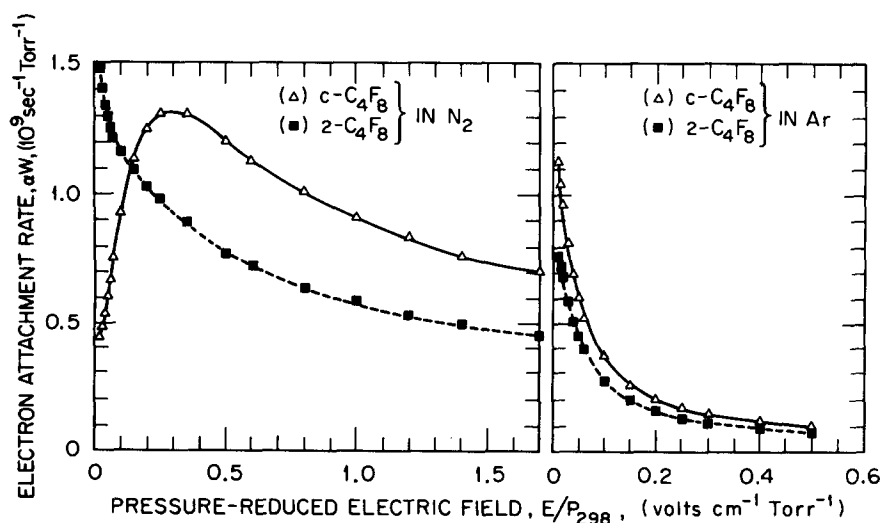


FIG. 4. Electron attachment rate αw vs E/P_{298} for $c\text{-C}_4\text{F}_8$ (Δ) and $2\text{-C}_4\text{F}_8$ (■) in N_2 and Ar.

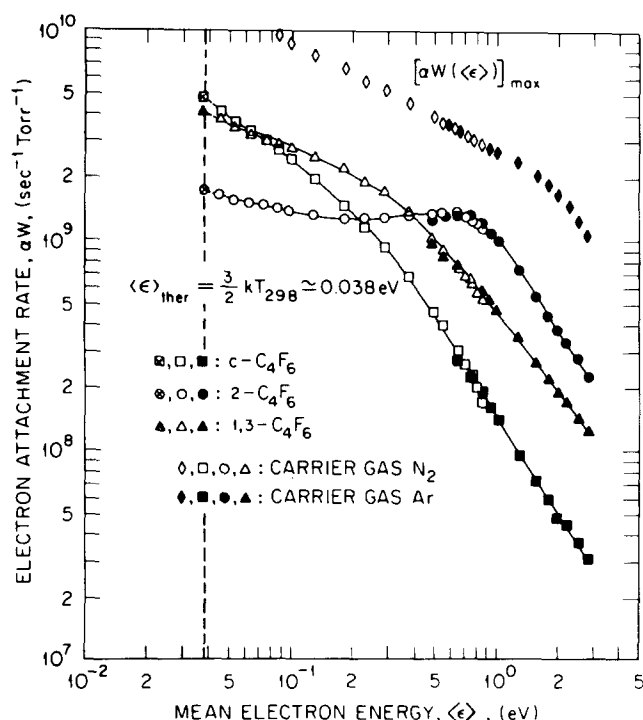


FIG. 5. Electron attachment rate αW vs $\langle \epsilon \rangle$ for $c\text{-C}_4\text{F}_8$ (\square , \blacksquare , and \circ), $2\text{-C}_4\text{F}_8$ (\circ , \bullet , and \otimes), and $1,3\text{-C}_4\text{F}_8$ (Δ , \blacktriangle , and \triangleleft) in N_2 ("open" points) and in Ar ("solid" points). The points \otimes , \bullet , and \blacktriangle correspond to the $(\alpha W)_{\text{ther}}$ values at $\langle \epsilon \rangle = \frac{3}{2} kT_{298} = 0.038 \text{ eV}$.

eV (Sec. III. E) is given for $c\text{-C}_4\text{F}_8$ (\otimes), $2\text{-C}_4\text{F}_8$ (\bullet) and $1,3\text{-C}_4\text{F}_8$ (\blacktriangle). A log-log plot was made to accommodate the wide range of values for both αW and $\langle \epsilon \rangle$.

A plot of αW vs $\langle \epsilon \rangle$ for $c\text{-C}_4\text{F}_8$ (\circ , \bullet) and $2\text{-C}_4\text{F}_8$ (Δ , \blacktriangle)

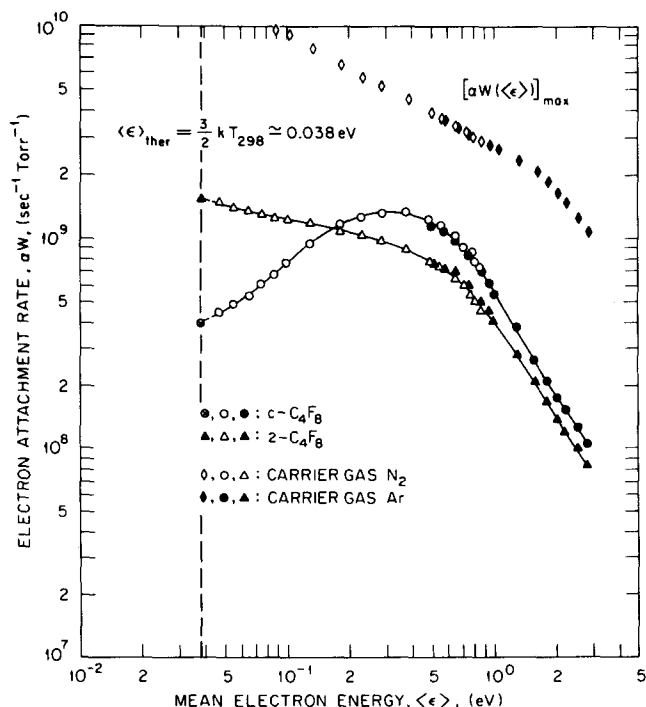


FIG. 6. Electron attachment rate αW vs $\langle \epsilon \rangle$ for $c\text{-C}_4\text{F}_8$ (\circ , \bullet , \otimes) and $2\text{-C}_4\text{F}_8$ (Δ , \blacktriangle , \triangleleft) in N_2 (open points) and Ar (solid points). The points \otimes and \blacktriangle correspond to the $(\alpha W)_{\text{ther}}$ values at $\langle \epsilon \rangle = \frac{3}{2} kT_{298} = 0.038 \text{ eV}$.

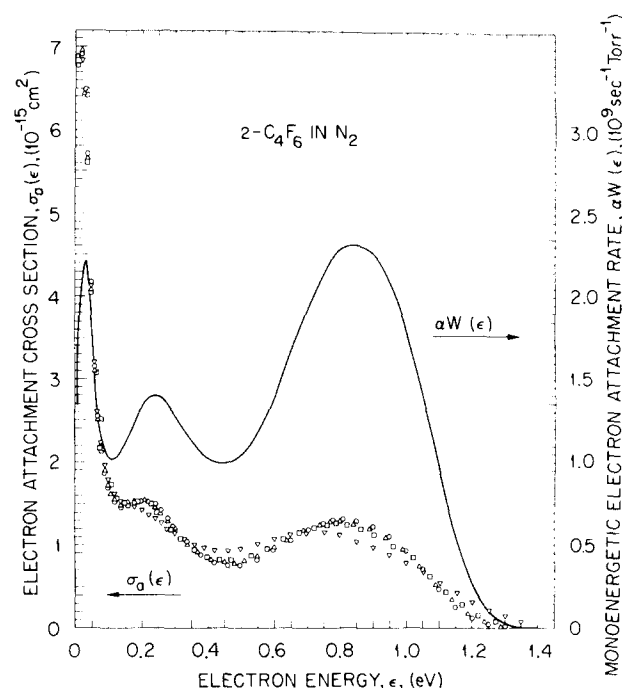


FIG. 7. Electron attachment cross section $\sigma_a(\epsilon)$ and monoenergetic electron attachment rate $\alpha W(\epsilon)$ as a function of electron energy ϵ for $2\text{-C}_4\text{F}_8$ in N_2 . $\sigma_a(\epsilon)$ after 495 iterations (∇ , $R = 6.5 \times 10^{-5}$), after 1386 iterations (\square , $R = 4.2 \times 10^{-5}$), after 1980 iterations (Δ , $R = 3.8 \times 10^{-5}$), and after 2970 iterations (\circ , $R = 3.5 \times 10^{-5}$).

is shown in Fig. 6. A similar notation was followed as in Fig. 5. In Fig. 6, the αW values for $c\text{-C}_4\text{F}_8$ and $2\text{-C}_4\text{F}_8$ in N_2 are averages of 4 and 11 runs, respectively, and in Ar averages of 4 and 8 runs, respectively. The $(\alpha W)_{\text{ther}}$ are also shown for $c\text{-C}_4\text{F}_8$ (\otimes) and $2\text{-C}_4\text{F}_8$ (\blacktriangle).

It is interesting to note that, although the attachment rates for the perfluorocarbons studied were measured independently in N_2 and Ar, the αW vs $\langle \epsilon \rangle$ plots for every molecule investigated in mixtures with the two carrier gases mesh well and form a continuous curve in the E/P range for which the $f(\epsilon, \langle \epsilon \rangle)$ overlap energy-wise, as seen in Figs. 5 and 6. Similar results were reported earlier^{7,8,16,17} (see also Part II).

D. Electron attachment cross section as a function of ϵ

The electron-swarm unfolding technique¹⁰ was applied to the present $\alpha W(\langle \epsilon \rangle)$ data for $c\text{-C}_4\text{F}_8$, $2\text{-C}_4\text{F}_8$, $1,3\text{-C}_4\text{F}_8$, $c\text{-C}_4\text{F}_8$, and $2\text{-C}_4\text{F}_8$ in N_2 , and the monoenergetic electron attachment rates $\alpha W(\epsilon)$ were obtained as a function of ϵ . From the so-determined $\alpha W(\epsilon)$ functions, $\sigma_a(\epsilon)$ were calculated through Eq. (3). A typical set of $\alpha W(\epsilon)$ and $\sigma_a(\epsilon)$ functions are given in Fig. 7 for $2\text{-C}_4\text{F}_8$. They were obtained after 2970 iterations (Sec. III. B). The various points for $\sigma_a(\epsilon)$ correspond to different numbers of iterations, as shown in the caption of Fig. 7. It is seen that the change in both the shape and the magnitude of $\sigma_a(\epsilon)$ is very small for large increases in the number of iterations showing convergence.

The $\sigma_a(\epsilon)$ for $c\text{-C}_4\text{F}_8$, $2\text{-C}_4\text{F}_8$, and $1,3\text{-C}_4\text{F}_8$ are shown in Fig. 8 and for $c\text{-C}_4\text{F}_8$ and $2\text{-C}_4\text{F}_8$ in Fig. 9, and are

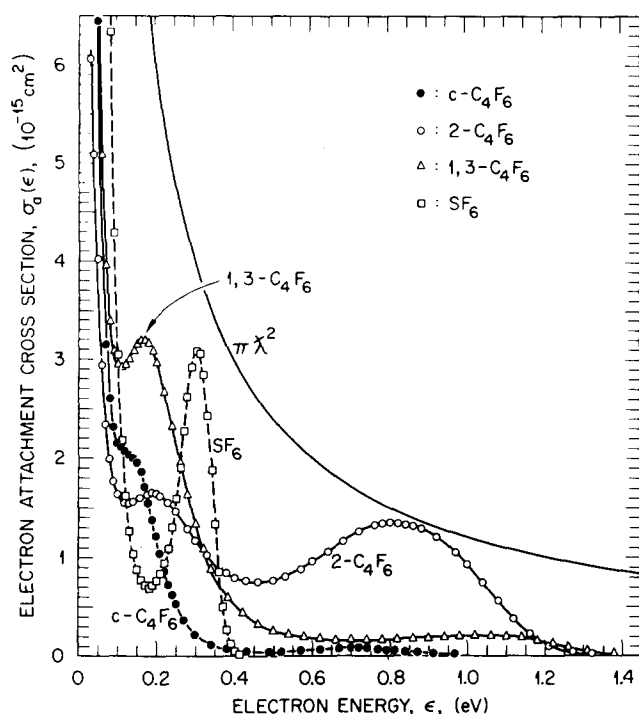


FIG. 8. Electron attachment cross section $\sigma_a(\epsilon)$ as a function of electron energy ϵ for $c\text{-C}_4\text{F}_6$ (\bullet), $2\text{-C}_4\text{F}_6$ (\circ), $1,3\text{-C}_4\text{F}_6$ (Δ), and SF_6 (\square). The maximum s -wave electron capture is represented by $\pi\chi^2$.

listed in Table IV. In Figs. 8 and 9, the $\sigma_a(\epsilon)$ functions for SF_6 and $\sigma_{a,\max} = \pi\chi^2$ are also shown for comparison.

The main features of the $\sigma_a(\epsilon)$ functions in Figs. 8 and 9 are (see also Table V) as follows:

- (1) For all PFC molecules except $c\text{-C}_4\text{F}_8$, $\sigma_a(\epsilon)$ in-

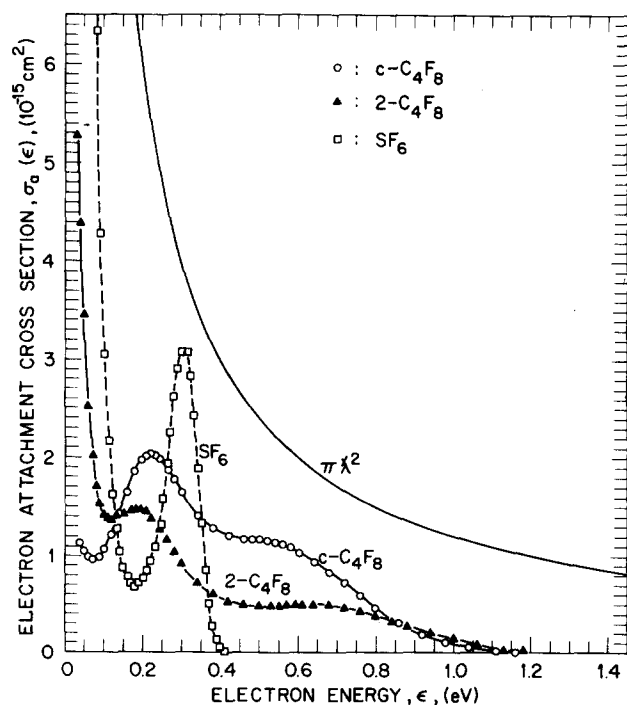


FIG. 9. Electron attachment cross section $\sigma_a(\epsilon)$ as a function of electron energy ϵ for $c\text{-C}_4\text{F}_8$ (\circ), $2\text{-C}_4\text{F}_8$ (\blacktriangle), and SF_6 (\square). The maximum s -wave electron capture is represented by $\pi\chi^2$.

TABLE IV. $\sigma_a(\epsilon)$ for $c\text{-C}_4\text{F}_6$, $2\text{-C}_4\text{F}_6$, $1,3\text{-C}_4\text{F}_6$, $c\text{-C}_4\text{F}_8$, and $2\text{-C}_4\text{F}_8$.

Electron energy ϵ (eV)	Electron attachment cross section $\sigma_a(\epsilon)$ (10^{-15} cm^2)				
	$c\text{-C}_4\text{F}_6$	$2\text{-C}_4\text{F}_6$	$1,3\text{-C}_4\text{F}_6$	$c\text{-C}_4\text{F}_8$	$2\text{-C}_4\text{F}_8$
0.04	9.57	5.09	10.00	1.13	4.40
0.06	4.23	2.94	5.08	0.99	2.52
0.08	2.60	1.99	3.38	0.97	1.71
0.10	2.16	1.64	2.94	1.07	1.42
0.12	2.06	1.55	2.95	1.23	1.37
0.14	2.00	1.56	3.08	1.43	1.40
0.16	1.85	1.60	3.19	1.65	1.44
0.18	1.55	1.63	3.15	1.86	1.47
0.20	1.22	1.63	2.97	1.98	1.45
0.22	0.89	1.59	2.66	2.03	1.38
0.24	0.63	1.51	2.32	1.99	1.28
0.26	0.44	1.40	1.97	1.89	1.16
0.28	0.30	1.29	1.64	1.78	1.04
0.30	0.21	1.17	1.34	1.64	0.92
0.34	0.11	0.97	0.89	1.42	0.72
0.38	0.07	0.84	0.60	1.29	0.60
0.42	0.05	0.77	0.44	1.21	0.53
0.46	0.047	0.75	0.33	1.18	0.50
0.50	0.046	0.77	0.26	1.16	0.48
0.55	0.053	0.84	0.22	1.13	0.49
0.60	0.062	0.96	0.19	1.00	0.49
0.65	0.068	1.09	0.17	0.92	0.48
0.70	0.073	1.21	0.17	0.78	0.47
0.75	0.070	1.30	0.17	0.62	0.43
0.80	0.058	1.35	0.16	0.46	0.37
0.85	0.041	1.32	0.17	0.32	0.31
0.90	0.028	1.24	0.18	0.23	0.25
0.95	0.017	1.11	0.19	0.15	0.19
1.00	0.008	0.93	0.20	0.09	0.13
1.05	0.003	0.69	0.20	0.05	0.08
1.10		0.46	0.19	0.024	0.045
1.15		0.25	0.17	0.009	0.020
1.20		0.12	0.14	0.003	0.007
1.25		0.04	0.10		0.002
1.30		0.011	0.06		
1.35		0.002	0.028		
1.40			0.011		
1.45			0.004		

creases with decreasing electron energy below 0.1 eV, attaining its maximum value at ~ 0 eV. At 0.04 eV, $\sigma_a(\epsilon)$ for $c\text{-C}_4\text{F}_8$, $2\text{-C}_4\text{F}_8$, $1,3\text{-C}_4\text{F}_8$, and $2\text{-C}_4\text{F}_8$ are very large ($\geq 5 \times 10^{-15} \text{ cm}^2$); at $\epsilon = 0.04$ eV, $\sigma_a(\epsilon)$ for $c\text{-C}_4\text{F}_8$ is $1.1 \times 10^{-15} \text{ cm}^2$.

(2) A well-defined second maximum in $\sigma_a(\epsilon)$ at $\sim 0.2 \pm 0.03$ eV is exhibited for $2\text{-C}_4\text{F}_8$, $1,3\text{-C}_4\text{F}_8$, $c\text{-C}_4\text{F}_8$, and $2\text{-C}_4\text{F}_8$. The $\sigma_a(\epsilon)$ for $c\text{-C}_4\text{F}_8$ exhibits a rather broad shoulder (extending from ~ 0.12 to ~ 0.16 eV) with a possible maximum at ~ 0.14 eV.

(3) A third broad maximum in $\sigma_a(\epsilon)$ is apparent for all PFC molecules at ~ 0.71 , 0.80 , 1.04 , 0.48 , and 0.59 eV for $c\text{-C}_4\text{F}_8$, $2\text{-C}_4\text{F}_8$, $1,3\text{-C}_4\text{F}_8$, $c\text{-C}_4\text{F}_8$, and $2\text{-C}_4\text{F}_8$, respectively. The peak in $\sigma_a(\epsilon)$ for $2\text{-C}_4\text{F}_8$ is the most dominant in this energy region. The peak cross section value for this molecule ($= 1.35 \times 10^{-15} \text{ cm}^2$) is close to $\sigma_{a,\max} = \pi\chi^2 = 1.50 \times 10^{-15} \text{ cm}^2$ ($\epsilon = 0.8$ eV).

(4) All five PFC molecules have much larger $\sigma_a(\epsilon)$ than SF_6 at $\epsilon \geq 0.4$ eV.

TABLE V. Electron attachment cross section maxima, values of $\sigma_a(\epsilon)$ at these maxima, energy integrated cross sections, autodetachment lifetimes of the parent negative ions at ~ 0.0 eV, and electron affinities for $c\text{-C}_4\text{F}_6$, $2\text{-C}_4\text{F}_6$, $1,3\text{-C}_4\text{F}_6$, $c\text{-C}_4\text{F}_8$, and $2\text{-C}_4\text{F}_8$.

Molecular formula	ϵ_2^a (eV)	$\sigma_a(\epsilon_2)$ (10^{-15} cm ²)	ϵ_3^a (eV)	$\sigma_a(\epsilon_3)$ (10^{-15} cm ²)	$\int_{0.04\text{ eV}}^{1.40\text{ eV}} \sigma_a(\epsilon) d\epsilon$ (10^{-15} eV cm ²)	$RI_{0.04\text{ eV}}^{1.40\text{ eV}}^b$ (%)	Lifetime of C_xF_y^- (μsec)	Electron affinity of C_xF_y (eV)
$c\text{-C}_4\text{F}_6$	~ 0.14	1.96	0.71	0.07	0.53	12.4	6.9 ^c 11.2 ^d	
$2\text{-C}_4\text{F}_6$	0.19	1.64	0.80	1.35	1.31	30.6	8.7 ^e 16.3 ^d	0.7–1.45 ^f
$1,3\text{-C}_4\text{F}_6$	0.17	3.19	1.04	0.20	1.07	25.2		
$c\text{-C}_4\text{F}_8$	0.22	2.03	0.48	1.21	0.98	23.1	12 ^c 14.8 ^g 200 ⁱ	$\geq 0.4^h$
$2\text{-C}_4\text{F}_8$	0.18	1.47	0.59	0.50	0.73	17.1	10.6 ^g 30.6 ^d	$\geq 0.7^h$

^a ϵ_2 and ϵ_3 give the energy position of the second and third maximum in $\sigma_a(\epsilon)$; the first maximum is at ~ 0.0 eV.^bSee Sec. III. F.^cW. T. Naff, C. D. Cooper, and R. N. Compton, J. Chem. Phys. **49**, 2784 (1968).^dJ. C. J. Thynne, Dyn. Mass Spectrom. **3**, 67 (1972).^eI. Sauers, L. G. Christophorou, and J. G. Carter (to be published).^fP. R. Hammond, J. Chem. Phys. **55**, 3468 (1971).^gP. W. Harland and J. C. J. Thynne, Int. J. Mass Spectrom. Ion Phys. **10**, 11 (1973).^hC. Lifshitz, T. O. Tiernan, and B. M. Hughes, J. Chem. Phys. **59**, 3182 (1973).ⁱJ. M. S. Henis and C. A. Mabie, J. Chem. Phys. **53**, 2999 (1970).

E. Thermal electron attachment rate $(\alpha w)_{\text{ther}}$

The $(\alpha w)_{\text{ther}}$ values for $c\text{-C}_4\text{F}_6$, $2\text{-C}_4\text{F}_6$, $1,3\text{-C}_4\text{F}_6$, $c\text{-C}_4\text{F}_8$, and $2\text{-C}_4\text{F}_8$ at $\langle\epsilon\rangle = 0.038$ eV, determined via Eq. (10), are shown in column 3 of Table VI and are plotted in Figs. 5 and 6.

If, for simplicity, we use a linear two-point extrapolation of the αw vs $\langle\epsilon\rangle$ plots for the first two measured αw values in N_2 (i. e., at $\langle\epsilon\rangle = 0.046$ and 0.054 eV), the $(\alpha w)_{\text{ther}}$ values so obtained for the five PFC molecules differ from those determined through the unfolding procedure by less than 3% (see Table VI).

TABLE VI. Thermal ($T = 298^\circ\text{K}$) rates for electron attachment to $c\text{-C}_4\text{F}_6$, $2\text{-C}_4\text{F}_6$, $1,3\text{-C}_4\text{F}_6$, $c\text{-C}_4\text{F}_8$, and $2\text{-C}_4\text{F}_8$.

Molecular formula	$(\alpha w)_{\text{meas.}}^a$ at $\langle\epsilon\rangle = 0.046$ eV ($10^9 \text{ sec}^{-1} \text{ torr}^{-1}$)	$(\alpha w)_{\text{ther., unf.}}^b$ at $\langle\epsilon\rangle = 0.038$ eV ($10^9 \text{ sec}^{-1} \text{ torr}^{-1}$)	$(\alpha w)_{\text{ther., extr.}}^c$ at $\langle\epsilon\rangle = 0.038$ eV ($10^9 \text{ sec}^{-1} \text{ torr}^{-1}$)	$(\alpha w)_{\text{ther., lit.}}^d$ ($10^9 \text{ sec}^{-1} \text{ torr}^{-1}$)
$c\text{-C}_4\text{F}_6$	4.20	4.89	4.72	4.54 ^e
$2\text{-C}_4\text{F}_6$	1.68	1.77	1.75	
$1,3\text{-C}_4\text{F}_6$	3.85	4.26	4.15	
				0.28 ^f 0.36 ^g
$c\text{-C}_4\text{F}_8$	0.45	0.40	0.41	0.39 ^g $\sim 0.7^h$
$2\text{-C}_4\text{F}_8$	1.48	1.56	1.56	1.59 ^g

^aPresent work. Measured αw values in N_2 for $E/P = 0.02 \text{ V cm}^{-1} \text{ torr}^{-1}$ ($\langle\epsilon\rangle = 0.046$ eV) at $T = 298^\circ\text{K}$.^bPresent work. Calculated thermal values from present unfolded $\alpha w(\epsilon)$ data, using Eq. (10).^cPresent work. Determined from two-point extrapolation to $\langle\epsilon\rangle = 0.038$ eV (Sec. III. E).^dReported thermal electron attachment rate constants (Sec. IV. E).^eK. M. Bansal and R. W. Fessenden, J. Chem. Phys. **59**, 1760 (1973).^fE. Schultes, Doctoral Thesis, Universität Bonn, Bonn, West Germany (1973); A. A. Christodoulides, E. Schultes, R. Schumacher, and R. N. Schindler, Z. Naturforsch. Teil A **29**, 389 (1974).^gF. J. Davis, R. N. Compton, and D. R. Nelson, J. Chem. Phys. **59**, 2324 (1973).^hL. G. Christophorou, D. L. McCorkle, and D. Pittman, J. Chem. Phys. **60**, 1183 (1974).

V. DISCUSSION

A. Electron attachment reaction mechanism

A large number of polyatomic molecules are known⁵ to attach electrons nondissociatively at low (≤ 2 eV) electron energies for times greater than 1 μ sec. For large and generally symmetric molecules, the excess energy of the captured electron is assumed to be distributed among the many vibrational degrees of freedom of the molecule for a time which is long enough for the negative ion to be detected in a time-of-flight mass spectrometer (TOFMS). Complete stabilization of the transient negative ion with the subsequent formation of a permanent negative ion is possible if the molecular electron affinity is positive (> 0 eV), and the time between collisions is small compared to the autodetachment lifetime τ_a .

The autodetachment lifetimes of $c\text{-C}_4\text{F}_8^*$, $2\text{-C}_4\text{F}_8^*$, $c\text{-C}_4\text{F}_8^+$, and $2\text{-C}_4\text{F}_8^+$ at ~ 0.0 eV were found¹⁸⁻²² in TOFMS studies to be > 1 μ sec (Table V). Although the lifetime of $1,3\text{-C}_4\text{F}_8^*$ has not yet been measured (it is under investigation²⁰), on the basis of the results on the other two isomers of C_4F_8 , it is expected to be > 1 μ sec also.

There is a lack of information on the electron affinities of the perfluorocarbons studied. A lower limit of ≥ 0.4 eV was, however, reported²³ for the electron affinity of $c\text{-C}_4\text{F}_8$ and of ≥ 0.7 eV for $2\text{-C}_4\text{F}_8$. In addition, from comparisons of the absorption onsets of charge transfer bands, it was concluded²⁴ that the electron affinities of O, $2\text{-C}_4\text{F}_8$, $2\text{-C}_4\text{F}_8$, and $c\text{-C}_4\text{F}_8$ should be in the order E.A.(O) $>$ E.A.($2\text{-C}_4\text{F}_8$) $>$ E.A.($2\text{-C}_4\text{F}_8$) $>$ E.A.($c\text{-C}_4\text{F}_8$). If we take as 1.46 eV the electron affinity of the oxygen atom²⁵ and use the lower limits²³ for $c\text{-C}_4\text{F}_8$ and $2\text{-C}_4\text{F}_8$, we predict $0.7 \leq \text{E.A.}(2\text{-C}_4\text{F}_8) \leq 1.46$ eV. It is reasonable to assume that the electron affinities of $c\text{-C}_4\text{F}_8$ and $1,3\text{-C}_4\text{F}_8$ are also positive.

A rough estimate of the average time τ_{col} between C_xF_y^* and N_2 collisions can be found from

$$\nu_{\text{col}} = v\sigma_L n_{\text{N}_2}, \quad (13)$$

where v is the relative velocity of C_xF_y^* and N_2 , n_{N_2} is

the number density of N_2 ($= N_0 P_{\text{N}_2} = 3.241 \times 10^{16} P_{\text{N}_2}$ at $T = 298$ °K), and σ_L is the classical Langevin expression for the cross section for spiralling collisions between C_xF_y^* and N_2 , given by^{26,27}

$$\sigma_L = \left(\frac{2\pi}{v} \right) \left(\frac{e^2 \alpha}{M_r} \right)^{1/2}. \quad (14)$$

In Eq. (14), α is the static polarizability of N_2 ($= 1.76 \times 10^{-24}$ cm³) (Ref. 28), e is the electronic charge, and M_r is the reduced mass for the system $\text{C}_x\text{F}_y^* - \text{N}_2$. From Eqs. (13) and (14), we have

$$\tau_{\text{col}} = \nu_{\text{col}}^{-1} = \frac{1}{2\pi N_0 P_{\text{N}_2}} \left(\frac{M_r}{e^2 \alpha_{\text{N}_2}} \right)^{1/2}. \quad (15)$$

For P_{N_2} equal to 500 and 2000 torr at $T = 298$ °K, Eq. (15) gives

$$\tau_{\text{col}} = 15.413 M_r^{1/2}, \quad \text{for 500 torr}, \quad (16)$$

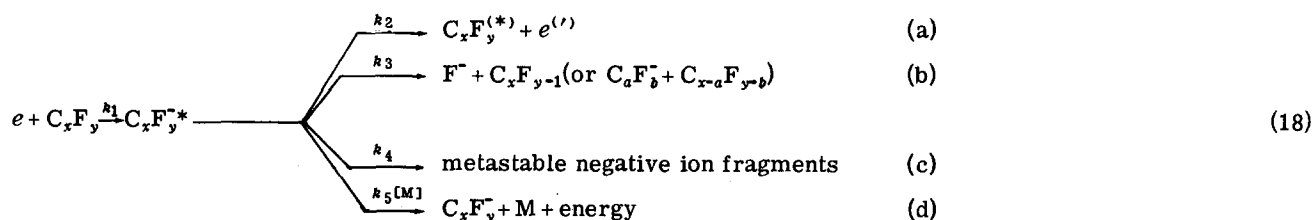
and

$$\tau_{\text{col}} = 3.853 M_r^{1/2}, \quad \text{for 2000 torr}, \quad (17)$$

where τ_{col} is given in sec, and M_r is expressed in g. From these calculations, τ_{col} was found equal to $\sim 10^{-10}$ sec [Eq. (16)] and $\sim 2.5 \times 10^{-11}$ sec [Eq. (17)] for the perfluorocarbons under consideration. Since the autodetachment lifetimes of the parent negative ions C_xF_y^* are $\geq 1 \times 10^{-6}$ sec, τ_{col} is smaller than τ_a by a factor of 10^4 to 10^5 .

The above findings coupled with the observation that the long-lived C_xF_y^* ions are mainly formed at ~ 0.0 eV in the TOFMS studies suggest that, in the present swarm study, low-energy electrons attach to the C_xF_y molecules nondissociatively, leading to the formation of permanent C_xF_y^- ions. Recent TOFMS results,²⁰ however, show that it is also possible that thermal and epithermal energy electrons can be captured by these molecules dissociatively. These studies show also that some of the fragment ions can themselves be metastable with $\tau_a > 10^{-6}$ sec.

We can summarize the decay channels of the low-lying negative ion resonances of the perfluorocarbons under discussion, as



The rate constants k_i in expressions (18) are as follows: k_1 for formation of C_xF_y^* , k_2 for autoionization, k_3 for dissociation, k_4 for formation of long-lived dissociation fragments, and $k_5[M]$ for collisional stabilization by a third body M (M = N_2 , Ar, or C_xF_y) (radiative stabilization may also occur). The symbol (*) indicates that C_xF_y^* may or may not retain as internal energy some

of the incident electron's kinetic energy and the symbol (') that the outgoing electron may carry less energy than the incident one.

The above reaction scheme (18) predicts

$$\alpha w(\langle \epsilon \rangle_j) = k_1 \frac{k_3 + k_4 + k_5[M]}{k_2 + k_3 + k_4 + k_5[M]}, \quad (19)$$

where $[M]$ is the concentration of M . Since $\tau_2 (= k_2^{-1})$ is very large ($> 1 \mu\text{sec}$) (the rate constant k_2 for autoionization is very small) and channel (18b) is pressure independent, $\alpha w(\epsilon)$ should be P independent, as is observed experimentally.

B. Negative-ion fragmentation of C_xF_y molecules

Negative ions produced by electron impact on the perfluorocarbons under discussion have been studied by several workers.^{3,20,29-34} It was generally found that "zero-energy" electron impacts result predominantly in the formation of long-lived parent negative ions $C_xF_y^-$, although fragment ions are also produced in many cases. For example, the TOFMS spectrum of $2-C_4F_8$ showed^{3,20} that the formation of $2-C_4F_8^-$ ions at ~ 0.0 eV contributes $> 98\%$ of all negative ions produced in the electron energy up to ~ 10 eV, with the remaining $< 2\%$ consisting of $C_3F_3^-$, F^- , and CF_3^- ions. A similar study^{3,20} for $2-C_4F_8$ showed that this molecule exhibits a far more extensive fragmentation than $2-C_4F_8$, with $\sim 96\%$ relative peak ion intensity for $2-C_4F_8^-$ at ~ 0.0 eV, $\sim 1\%$ for $C_4F_7^-$ at ~ 0.0 eV, and $\sim 3\%$ for F^- , $C_3F_5^-$, $C_4F_6^-$, CF_3^- , $C_3F_3^-$, and $C_2F_3^-$ at higher than zero energies (up to ~ 5.4 eV). The observation³⁴ of $C_4F_7^-$ from $2-C_4F_8$ at ~ 0 eV is in accord with the findings of Sauers *et al.*²⁰ A series of nine dissociative capture peaks from $c-C_4F_8$ leading to F^- (five peaks), CF_3^- , $C_2F_3^-$, and $C_3F_5^-$ (two peaks) with maxima located from 1.75 to 10.5 eV, in addition to the nondissociative capture peak at 0.03 eV for the formation of $c-C_4F_8^-$, were observed³⁴ and were ascribed to a series of negative ion states.

The higher members of the alicyclic and aromatic series, notably those containing methyl side groups, such as $c-C_6F_{12}$ and $c-C_7F_{14}$, were found³³ to undergo extensive fragmentation, although the formation of the parent negative ions remained high.

C. Electron attachment cross sections

The electron attachment cross section for $c-C_4F_8$ showed three maxima (Fig. 9) in the energy range ~ 0 to ~ 1.5 eV: a "zero-energy" peak with $\sigma_a(\epsilon = 0.03 \text{ eV}) = 1.17 \times 10^{-15} \text{ cm}^2$, a dominant peak at 0.22 eV with $\sigma_a(\epsilon = 0.22 \text{ eV}) = 2.03 \times 10^{-15} \text{ cm}^2$, and a broad shoulder extending from 0.4 to 0.6 eV with $\sigma_a(\epsilon = 0.5 \text{ eV}) \approx 1.16 \times 10^{-15} \text{ cm}^2$. Similar results were found for $c-C_4F_8$, $2-C_4F_8$, $1,3-C_4F_8$ (Fig. 8), and $2-C_4F_8$ (Fig. 9 and Table V).

The formation of negative ions from $c-C_4F_8$ at low-electron energies has been studied by several workers.^{21,29-32} The energy dependence of the total electron attachment cross section showed³⁰ a complicated structure in the energy range from ~ 0 to 12 eV, with the largest cross section value ($= 2.14 \times 10^{-17} \text{ cm}^2$) at the resonance maximum close to 0 eV. The $C_4F_8^-$ ion current was not normalized, however, by the electron current which considerably underestimates¹⁸ the reported³⁰ $\sigma_a(\epsilon)$, and the absence of a mass analysis of the ions formed hinders the interpretation of these data. The $c-C_4F_8^-$ ion was found²¹ to be formed at ~ 0 eV. This ion was responsible for virtually all of the ion current intensity measured. The observed²¹ symmetrical

resonance peak reached a maximum value at 0.45 ± 0.1 eV. Based on the relative peak intensities of $c-C_4F_8^-$ and SF_6^- and a value for the electron attachment cross section for SF_6 at $\epsilon = 0.05$ eV equal to $1.17 \times 10^{-14} \text{ cm}^2$,³⁵ it was estimated²¹ that $\sigma_{c-C_4F_8}(\epsilon = 0.05 \text{ eV}) = 1.3 \times 10^{-16} \text{ cm}^2$. This estimate is an order of magnitude smaller than the value of $1.06 \times 10^{-15} \text{ cm}^2$ at $\epsilon = 0.05$ eV from the present work.

The energy dependence of $\sigma_a(\epsilon)$ for $c-C_4F_8$, $2-C_4F_8$, $1,3-C_4F_8$, $c-C_4F_8$, and $2-C_4F_8$ (Figs. 8 and 9) showed three negative ion resonances at electron energies below ~ 1.3 eV. Many molecules were found to possess a multiplicity of negative ion resonances in the subexcitation energy region. This was clearly illustrated by the recent data¹⁴ on the production of Cl^- from chloroethylenes and chloroethanes. For both groups of molecules, five negative ion states were identified¹⁴ below ~ 2 eV and were associated with orbitals dominated by the p orbitals of the chlorine atoms.

It is interesting to compare the $\sigma_a(\epsilon)$ for $c-C_4F_8$, $2-C_4F_8$, $1,3-C_4F_8$, $c-C_4F_8$, and $2-C_4F_8$ with that for SF_6 . The $\sigma_a(\epsilon)$ for the former extend to much higher energies than the $\sigma_a(\epsilon)$ for SF_6 , which drops sharply above ~ 0.4 eV (Figs. 8 and 9). This behavior of $\sigma_a(\epsilon)$ as a function of ϵ seems to explain some features of the breakdown strength behavior of SF_6 in comparison to that of the perfluorocarbons. The breakdown strength of the five PFC studied was found¹⁻⁴ to be 1.4 to 2.2 times larger than that for SF_6 under similar experimental conditions, and to hold better in nonuniform fields than that for SF_6 (see discussion in Refs. 1 to 4 and Part II).

D. Thermal electron attachment rates

Thermal electron attachment rate constants k_{ther} (in $\text{cm}^3 \text{sec}^{-1} \text{molecule}^{-1}$) for $c-C_4F_8$, $c-C_4F_8$, and $2-C_4F_8$ were determined by a microwave conductometric method combined with the pulse radiolysis technique and were found³⁶ equal to 1.4×10^{-7} , 1.2×10^{-8} , and $4.9 \times 10^{-8} \text{ cm}^3 \text{sec}^{-1} \text{molecule}^{-1}$, respectively, in mixtures with propane at 25°C . To convert these thermal rate constants to thermal attachment rates $(\alpha w)_{\text{ther}}$, the following well-known relationship [equivalent to Eq. (1)] is used

$$\alpha w = N_0 \int_0^\infty v \sigma_a(v) f(v) dv = N_0 \langle v \sigma_a(v) \rangle \equiv N_0 k \quad (20)$$

or

$$(\alpha w)_{\text{ther}} = 3.241 \times 10^{16} k_{\text{ther}} (\text{in sec}^{-1} \text{ torr}^{-1}) \quad (21)$$

at $T = 298^\circ\text{K}$. The values of $(\alpha w)_{\text{ther}}$ obtained from Eq. (21) by using the literature data³⁶ on k_{ther} for $c-C_4F_8$, $c-C_4F_8$, and $2-C_4F_8$ are compared in Table VI with the present measurements for these molecules and are seen to be in excellent agreement.

A modified time-of-flight electron swarm method, called the drift-dwell-drift technique, was used³⁷ to obtain k_{ther} for $c-C_4F_8$ which was found equal to $1.11 \times 10^{-8} \text{ cm}^3 \text{sec}^{-1} \text{molecule}^{-1}$ ($= 2.6 \times 10^8 \text{ sec}^{-1} \text{ torr}^{-1}$). From time-dependent measurements at constant electron scavenger concentration, a k_{ther} value of $0.9 \times 10^{-8} \text{ cm}^3 \text{sec}^{-1} \text{molecule}^{-1}$ ($= 2.92 \times 10^8 \text{ sec}^{-1} \text{ torr}^{-1}$) was re-

ported^{38,39} for $c\text{-C}_4\text{F}_8$ by using the electron cyclotron resonance (ECR) technique. Since the present and the reported thermal values of the electron attachment rate are averages over several runs at various pressures, the agreement of all the data is considered to be good. No such data were found in the literature for $2\text{-C}_4\text{F}_8$ and $1,3\text{-C}_4\text{F}_8$.

An earlier electron swarm study⁴⁰ of $c\text{-C}_4\text{F}_8$ in N_2 at 400 torr gave $(\alpha w)_{\text{ther}} \approx 7 \times 10^8 \text{ sec}^{-1} \text{ torr}^{-1}$, which is higher than the present ($\approx 4 \times 10^8 \text{ sec}^{-1} \text{ torr}^{-1}$) value. It is noted, however, that the overall energy dependence of αw and the position of the maxima of the $\alpha w(\epsilon)$ and $\sigma(\epsilon)$ functions are in excellent agreement with the present work. It is believed that the discrepancy (by a factor of ~ 1.5) in the magnitude of the $\alpha w(\epsilon)$ functions between the earlier⁴⁰ and the present data is due to an error in the measurement of the pressure of $c\text{-C}_4\text{F}_8$ in the earlier study.⁴⁰

E. Effect of molecular structure on the electron attachment to perfluorocarbons

1. Open-chain saturated PFC molecules

Observations of electron attachment to the saturated perfluorocarbons CF_4 ,^{37,41} C_2F_6 ,^{37,41} C_3F_8 ,^{37,41,42} and $n\text{-C}_4\text{F}_{10}$ (Ref. 41) with an open-chain structure shows that their thermal attachment rates are several orders of magnitude smaller than those measured for the PFC molecules studied in this and the following paper. The $(\alpha w)_{\text{ther}}$ was reported^{37,41,42} to be $< 10^3 \text{ sec}^{-1} \text{ torr}^{-1}$ for CF_4 and C_2F_6 , $\leq 10^4 \text{ sec}^{-1} \text{ torr}^{-1}$ for C_3F_8 , and $\sim 3 \times 10^5 \text{ sec}^{-1} \text{ torr}^{-1}$ for $n\text{-C}_4\text{F}_{10}$. As the molecular size (chain length) increases, $(\alpha w)_{\text{ther}}$ increases.

It should be noted here, however, that although $(\alpha w)_{\text{ther}}$ for the above saturated PFC molecules are very small, they may be significantly larger at higher electron energies. This is the case for C_3F_8 for which the electron attachment rate increases by a factor of $\sim 10^2$ in going from thermal energy to $\langle \epsilon \rangle = 0.85 \text{ eV}$. Thus, for a complete picture of the electron scavenging efficiency of a molecule, it is necessary that the dependence of the attachment rate and cross section on the electron energy is studied.

It seems from the above findings that, as the molecular structure becomes more symmetric and compact in open-chain saturated perfluorocarbons (i. e., in going from $n\text{-C}_4\text{F}_{10}$ to CF_4), the electron capturing efficiency decreases.

2. Open-chain unsaturated PFC molecules

With the introduction of double or triple bonds in the chain of the saturated perfluorocarbons, $\alpha w(\epsilon)$ increases drastically. Thus, the one double-bonded $2\text{-C}_4\text{F}_8$, the two double-bonded $1,3\text{-C}_4\text{F}_8$, and the one triple-bonded $2\text{-C}_4\text{F}_8$ showed significant increases in the thermal electron attachment rate, reaching values of up to $4 \times 10^9 \text{ sec}^{-1} \text{ torr}^{-1}$.

The $(\alpha w)_{\text{ther}}$ for the unsaturated double-bonded C_2F_4 was reported⁴¹ to be larger by a factor of $\sim 10^4$ than that for the saturated single-bonded C_2F_6 compound although

the observed large $(\alpha w)_{\text{ther}}$ value ($\sim 1 \times 10^5 \text{ sec}^{-1} \text{ torr}^{-1}$) for C_2F_4 might be due⁴¹ to impurities. No other electron attachment data on open-chain unsaturated perfluorocarbons seem to exist.

3. Cyclic PFC molecules

In this category of perfluorocarbons, we include three-, four-, five-, and six-carbon ring molecules, with or without double bonds. The present work (see also Part II) indicates that the introduction of double bonds in cyclic perfluorocarbons is not so significant as in the open-chain unsaturated PFC molecules. For example, $c\text{-C}_4\text{F}_8$ with one double bond and $c\text{-C}_4\text{F}_8$ with only single bonds did not show appreciable differences in the magnitude of the electron attachment rate in the energy range studied.

A reported³⁶ lower limit ($< 1 \times 10^3 \text{ sec}^{-1} \text{ torr}^{-1}$) for $(\alpha w)_{\text{ther}}$ for the cyclic $c\text{-C}_3\text{F}_8$ is low compared to the $(\alpha w)_{\text{ther}}$ values (between 4×10^8 and $2 \times 10^{10} \text{ sec}^{-1} \text{ torr}^{-1}$) for the cyclic perfluorocarbons $c\text{-C}_4\text{F}_8$, $c\text{-C}_4\text{F}_8$, $c\text{-C}_5\text{F}_8$, $c\text{-C}_6\text{F}_{10}$, $c\text{-C}_6\text{F}_{12}$, C_7F_8 , and C_8F_{16} of the present and the following (Part II) paper.

- ¹L. G. Christophorou, D. R. James, R. Y. Pai, R. A. Mathis, M. O. Pace, D. W. Bouldin, A. A. Christodoulides, and C. C. Chan, High Voltage Research, Semiannual Report, ORNL/TM-6113, November 1977.
- ²L. G. Christophorou, Proceedings of XIIIth International Conference on Phenomena in Ionized Gases, Berlin, G.D.R., 12-17 September 1977, Invited Lectures, p. 51.
- ³D. R. James, L. G. Christophorou, R. Y. Pai, M. O. Pace, R. A. Mathis, I. Sauers, and C. C. Chan, Proceedings of the 1st International Symposium on Gaseous Dielectrics, Knoxville, TE, 6-8 March 1978, Oak Ridge National Laboratory Report CONF-780301, p. 224.
- ⁴L. G. Christophorou, D. R. James, R. Y. Pai, R. A. Mathis, I. Sauers, M. O. Pace, D. W. Bouldin, A. A. Christodoulides, and C. C. Chan, High Voltage Research, Semiannual Report, ORNL/TM-6384, June 1978.
- ⁵L. G. Christophorou, *Atomic and Molecular Radiation Physics* (Wiley-Interscience, New York, 1971).
- ⁶J. F. Rademacher, Ph.D. thesis, University of Tennessee, Knoxville (1974).
- ⁷A. A. Christodoulides and L. G. Christophorou, ORNL/TM-3163 (1970).
- ⁸L. G. Christophorou, E. L. Chaney, and A. A. Christodoulides, Chem. Phys. Lett. 3, 363 (1969).
- ⁹L. G. Christophorou, R. N. Compton, G. S. Hurst, and P. W. Reinhardt, J. Phys. Chem. 43, 4273 (1965).
- ¹⁰L. G. Christophorou, D. L. McCorkle, and V. E. Anderson, J. Phys. B 4, 1163 (1971).
- ¹¹A. S. Davydov, *Quantum Mechanics* (Pergamon, New York, 1965), Chap. XI.
- ¹²L. G. Christophorou, Chem. Rev. 76, 409 (1976).
- ¹³L. G. Christophorou and R. P. Blaunstein, Chem. Phys. Lett. 12, 173 (1971).
- ¹⁴J. P. Johnson, L. G. Christophorou, and J. G. Carter, J. Chem. Phys. 67, 2196 (1977).
- ¹⁵In the present work, new values of the mean electron energy $\langle \epsilon \rangle$ in N_2 were numerically computed for the lower E/P_{298} range. These are 0.046, 0.054, and 0.064 eV for $E/P_{298} = 0.02, 0.03, \text{ and } 0.04 \text{ V cm}^{-1} \text{ torr}^{-1}$, respectively. They replace the values of 0.038, 0.052, and 0.063 eV, respectively, at the same E/P_{298} values used previously at this laboratory.
- ¹⁶E. L. Chaney, L. G. Christophorou, P. M. Collins, and

- J. G. Carter, *J. Chem. Phys.* **52**, 4413 (1970).
- ¹⁷A. A. Christodoulides and L. G. Christophorou, *J. Chem. Phys.* **54**, 4691 (1970).
- ¹⁸W. T. Naff, C. D. Cooper, and R. N. Compton, *J. Chem. Phys.* **49**, 2784 (1968).
- ¹⁹J. C. J. Thynne, *Dyn. Mass Spectrom.* **3**, 67 (1972).
- ²⁰I. Sauers, L. G. Christophorou, and J. G. Carter (to be published).
- ²¹P. W. Harland and J. C. J. Thynne, *Int. J. Mass Spectrom. Ion Phys.* **10**, 11 (1973).
- ²²J. M. S. Henis and C. A. Mabie, *J. Chem. Phys.* **53**, 2999 (1970).
- ²³C. Lifshitz, T. O. Tiernan, and B. M. Hughes, *J. Chem. Phys.* **59**, 3182 (1973).
- ²⁴P. R. Hammond, *J. Chem. Phys.* **55**, 3468 (1971).
- ²⁵See reported values of E.A.(O) in Ref. 5, p. 547.
- ²⁶E. W. McDaniel, *Collision Phenomena in Ionized Gases* (Wiley, New York, 1964).
- ²⁷R. E. Goans and L. G. Christophorou, *J. Chem. Phys.* **60**, 1036 (1974).
- ²⁸H. H. Landolt and R. Börnstein, *Zahlenwerte und Functionen (Tables on Chemical Data)*, (Springer, Berlin, 1951), Vol. 1, p. 510.
- ²⁹R. M. Reese, V. H. Dibeler, and F. L. Mohler, *J. Res. Natl. Bur. Stand.* **57**, 367 (1956).
- ³⁰M. V. Kurepa, Third Czechoslovak Conference on Electronics and Vacuum Physics Transactions, Prague, Czechoslovakia, (1965), p. 107.
- ³¹M. M. Bibby and G. Carter, *Trans. Faraday Soc.* **62**, 2637 (1966).
- ³²C. Lifshitz, *Isr. J. Chem.* **6**, 847 (1968).
- ³³C. Lifshitz, A. M. Peers, R. Grajower, and M. Weiss, *J. Chem. Phys.* **53**, 4605 (1970).
- ³⁴C. Lifshitz and R. Grajower, *Int. J. Mass Spectrom. Ion Phys.* **10**, 25 (1973).
- ³⁵L. G. Christophorou, D. L. McCorkle, and J. G. Carter, *J. Chem. Phys.* **54**, 253 (1971).
- ³⁶K. M. Bansal and R. W. Fessenden, *J. Chem. Phys.* **59**, 1760 (1973).
- ³⁷F. J. Davis, R. N. Compton, and D. R. Nelson, *J. Chem. Phys.* **59**, 2324 (1973).
- ³⁸E. Schultes, Ph.D. thesis, Universität Bonn, Bonn, West Germany (1973).
- ³⁹A. A. Christodoulides, E. Schultes, R. Schumacher, and R. N. Schindler, *Z. Naturforsch. Teil A* **29**, 389 (1974).
- ⁴⁰L. G. Christophorou, D. L. McCorkle, and D. Pittman, *J. Chem. Phys.* **60**, 1183 (1974).
- ⁴¹R. W. Fessenden and K. M. Bansal, *J. Chem. Phys.* **53**, 3468 (1970).
- ⁴²L. G. Christophorou, D. R. James, R. Y. Pai, M. O. Pace, R. A. Mathis, D. W. Bouldin, and D. E. Tittle, High Voltage Research, ORNL/TM-5806, February 1977.